European Neuropsychopharmacology (2019) 29, 195–210

www.elsevier.com/locate/euroneuro

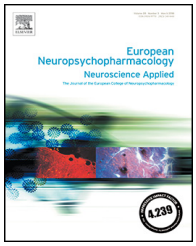

Effect of chronic methylphenidate treatment on hippocampal neurovascular unit and memory performance in late adolescent rats

Vanessa Coelho-Santos[a,b], Filipa L. Cardoso[a,b], Ana Magalhães[c], Margarida Ferreira-Teixeira[a,b], Ricardo A. Leitão[a,b,d], Célia Gomes[a,b,d], Manuel Rito[e], Marcos Barbosa[b,d,e], Carlos A. Fontes-Ribeiro[a,b,d], Ana Paula Silva[a,b,d,*]

[a] *Faculty of Medicine, Institute of Pharmacology and Experimental Therapeutics, University of Coimbra, Azinhaga de Santa Comba, Celas, 3000-548, Coimbra, Portugal*
[b] *Faculty of Medicine, Coimbra Institute for Clinical and Biomedical Research (iCBR), University of Coimbra, Portugal*
[c] *Addiction Biology Group, Instituto de Investigação e Inovação em Saúde (i3S), Universidade do Porto, Porto, Portugal*
[d] *CNC.IBILI Consortium, University of Coimbra, Coimbra, Portugal*
[e] *Neurosurgery Service, Coimbra Hospital and University Centre (CHUC), Coimbra, Portugal*

Received 8 May 2018; received in revised form 13 November 2018; accepted 1 December 2018

KEYWORDS
ADHD;
Astrocytes;
Blood-brain barrier;
Methylphenidate;
Oxidative stress;
Working memory

Abstract
Methylphenidate (MPH) is the classic treatment for attention deficit hyperactivity disorder (ADHD) among children and adults. Despite its beneficial effects, non-medical use of MPH is nowadays a problem with high impact on society. Thus, our goal was to uncover the neurovascular and cognitive effects of MPH chronic use during a critical period of development in control conditions. For that, male Wistar Kyoto rats were treated with MPH (1.5 or 5 mg/kg/day at weekdays, per os) from P28 to P55. We concluded that the higher dose of MPH caused hippocampal blood-brain barrier (BBB) hyperpermeability by vesicular transport (transcytosis) concomitantly with the presence of peripheral immune cells in the brain parenchyma. These

* Corresponding author at: Faculty of Medicine, Institute of Pharmacology and Experimental Therapeutics, University of Coimbra, Azinhaga de Santa Comba, Celas, 3000-548, Coimbra, Portugal.
E-mail addresses: apmartins@fmed.uc.pt, apsilva@cnc.cj.uc.pt (A.P. Silva).

https://doi.org/10.1016/j.euroneuro.2018.12.007

observations were confirmed by *in vitro* studies, in which the knockdown of caveolin-1 in human brain endothelial cells prevented the increased permeability and leukocytes transmigration triggered by MPH (100 μM, 24 h). Furthermore, MPH led to astrocytic atrophy and to a decrease in the levels of several synaptic proteins and impairment of AKT/CREB signaling, together with working memory deficit assessed in the Y-maze test. On the contrary, we verified that the lower dose of MPH (1.5 mg/kg/day) increased astrocytic processes and upregulated several neuronal proteins as well as signaling pathways involved in synaptic plasticity culminating in working memory improvement. In conclusion, the present study reveals that a lower dose of MPH in normal rats improves memory performance being associated with the modulation of astrocytic morphology and synaptic machinery. However, a higher dose of MPH leads to BBB dysfunction and memory impairment.

1. Introduction

Methylphenidate (MPH) is the first line treatment for attention deficit hyperactivity disorder (ADHD), one of the most common neuropsychiatric disorders of childhood (Sharma and Couture, 2014). Despite evidence for improvement of ADHD behavioral and neurocognitive impairment with MPH, its prescription among children is still controversial. Additionally, there is currently a concern about MPH use for cognitive enhancement (Urban and Gao, 2014) that together with ADHD misdiagnosis problematic have raised an intense debate. The underlying mechanisms contributing to the effectiveness of MPH have also received little attention besides its role on dopaminergic system. In this context, chronic MPH use during development can modulate genes and transcription factors associated with long-term potentiation, synaptogenesis and synaptic plasticity (Andersen et al., 2002). Importantly, the use of MPH under non-pathological conditions may have abuse potential since it will interact with the same brain pathways activated by other psychostimulants, such as amphetamine, methamphetamine and cocaine (Volkow et al., 2002). Therefore, non-medical consumption of MPH is nowadays a major public health concern.

Blood-brain barrier (BBB) is a selective and dynamic structure that separates the central nervous system (CNS) from the periphery by restricting immune cells access to the brain (Cecchelli et al., 2007) and by sustaining a stable environment for neural function (Cardoso et al., 2010). The core anatomical element of the BBB is the microvascular endothelium formed by endothelial cells (ECs) that are associated with pericytes, basal lamina, astrocytes, microglia and neurons forming the neurovascular unit (NVU). The adherens (AJs) and tight junctions (TJs) between adjacent ECs regulate the paracellular permeability, while the transcellular route can occur through caveolae vesicles that are dynamic pieces of membrane composed by the structural protein caveolin-1 (Cav1) and enriched in cholesterol and sphingolipids (Fernandez et al., 2002).

BBB alterations are likely involved in all neurodegenerative diseases and are also known to occur in drug abuse conditions (Dietrich, 2009; Sajja et al., 2016). In fact, psychostimulants use, such as cocaine and methamphetamine, are often associated with BBB breakdown leading to the extravasation of peripheral cells and components into the brain parenchyma that in turn will originate neuroinflammation, oxidative stress, edema, excitotoxicity, and neurodegeneration (Kousik et al., 2012; Coelho-Santos et al., 2015; Sajja et al., 2016; Gonçalves et al., 2017; Leitão et al., 2018). These events usually drive to a multitude of pathophysiological responses that further exacerbate the initial trigger. MPH has also been demonstrated to affect blood flow in different brain regions (Marquand et al., 2012) and capillary wall structural changes (Bahcelioglu et al., 2009). Accordingly, we previously showed that MPH promotes human brain endothelial permeability by interfering with the caveolae-dependent vesicular transport (Coelho-Santos et al., 2016). Additionally, we recently unraveled the differences between the chronic impact of MPH on brain immune privilege in the prefrontal cortex of healthy and ADHD rats MPH promoted cortical BBB permeability and both neuroinflammatory and oxidative responses in control rats, whereas in ADHD conditions, a lower dose of MPH had a beneficial (Coelho-Santos et al., 2018).

Following our previous work, we now hypothesized that MPH use under control conditions could compromise hippocampal BBB integrity disrupting the immune privileged status of the CNS and leading to neuronal damage and cognitive deficits. In fact, hippocampus is critical for memory processes (Bird and Burgess, 2008; Urban and Gao, 2014) and seems to be very susceptible to psychostimulants use (Martins et al., 2011). Thus, our aim was to unravel the effect of chronic MPH use on hippocampal NVU and memory performance in healthy rats to simulate a non-medical use of MPH or misdiagnosis, and also to clarify its cellular effects by using an *in vitro* BBB model.

2. Experimental procedures

2.1. Animals and treatments

Male Wistar Kyoto rats (WKY; arrived at 24 days-old; ~55 g body weight; Charles River Laboratories, France) were housed under controlled environmental conditions (12 h light:dark cycle, 24 ± 1 °C) with food and water *ad libitum*.

Animals were divided in three different groups: control group (vehicle, tap water), 1.5 mg/kg/day MPH group (MPH 1.5) and 5 mg/kg/day MPH group (MPH 5) (Sigma-Aldrich, USA). Given the existing differences in the metabolism of rodents *versus* humans, a higher dose of a drug (approx.

3-fold) is usually required to achieve blood levels in rats within the range found in humans (Gerasimov et al., 2000). Clinical use of MPH for ADHD treatment in children typically involves oral administration of doses around 0.25–1.0 mg/kg, which result in peak plasma levels of MPH in the 8–40 ng/mL range (Swanson and Volkow, 2002). Both MPH doses used in our study ensured that therapeutically relevant plasma drug levels were achieved and mimic the dosage range in humans (Harvey et al., 2011; Somkuwar et al., 2013). Noteworthy, these same doses were previously used by us (Coelho-Santos et al., 2018).

Individual administration was performed by gavage during the morning from Monday to Friday between postnatal days (P)28-P55 (4 weeks), equivalent to late-childhood through late-adolescence in humans (Marco et al., 2011). Behavioral tests were performed at P56, and animals were sacrificed after 24 h (P57). The number of animals used in each experiment are indicated in figure legends and the total number of Wistar Kyoto rats used in the present study were 42. All experiments were performed by certified researchers in accordance with European Community Council Directives (2010/63/EU) and Portuguese law for care and use of experimental animals (DL n° 113/2013). This study was approved by the Institutional Animal Care and Use Committee (FMUC/CNC, University of Coimbra, Portugal) and Portuguese National Authority for Animal Health "DGAV". All efforts were made to minimize animal suffering and to reduce the number of animals used.

2.2. Immunohistochemistry

Rats were anaesthetized with an intraperitoneal injection of ketamine (50 mg/kg), xylazine (10 mg/kg) and transcardially perfused with 4% paraformaldehyde (PFA; Sigma-Aldrich) in 0.01 M phosphate buffered saline (PBS, pH 7.4). Brains were post fixed and immunolabelling was performed as previously described (Coelho-Santos et al., 2018). For albumin, collagen IV, CD169, CD45, metalloproteinase (MMP)-9 and anti-3-nitrotyrosine (3-NT) we used slices with 14 μm. Free-floating slices with 50 μm were co-stained against glial fibrillary acidic protein (GFAP; astrocytic marker) and cluster of differentiation 31 (CD31 or PECAM-1; endothelial marker).

Primary antibodies used are indicated in Supplemental Table S1. Images were recorded using LSM 710 Meta Confocal microscope (Carl Zeiss). Quantification of fluorescence and co-localization were determined using the FIJI J software (NIH, USA). GFAP-labeled astrocytes were analyzed using the NeuronJ program, a plugin of FIJI Software (Leitão et al., 2018).

2.3. Western blot analysis

After anesthesia, rats were and transcardially perfused with 0.01 M PBS, pH 7.4. Western blots were performed as previously described by us (Coelho-Santos et al., 2018) and primary antibodies are listed in Supplemental Table S1.

2.4. Transmission electron microscopy

Rats were anesthetized and transcardially perfused with 4% PFA. Hippocampi (1-mm pieces) were immersed in 2.5% glutaraldehyde in 0.1 M sodium cacodylate buffer (pH 7.2) for 2 h. Post-fixation was performed using 1% osmium tetroxide for 1 h 30 min. Afterwards, 1% aqueous uranyl acetate was added for 1 h in the dark, for contrast enhancement. Samples were dehydrated in a graded ethanol series (30–100%), impregnated and embedded in Epoxy resin (Fluka Analytical, USA). Ultrathin sections (70 nm) were mounted on copper grids and stained with 0.2% lead citrate for 7 min. Observations were carried out on a FEI-Tecnai G2 Spirit Bio Twin at 100 kV.

2.5. Quantification of reactive oxygen species (ROS)

ROS assay was performed as previous published by us (Coelho-Santos et al., 2018). Briefly, serum or hippocampi lysates were added to 0.1 M sodium acetate buffer (pH 4.8) at 37 °C in a 96-well plate. Samples were taken and 100 μL of the mixed N,N-Diethyl-p-phenylenediamine (DEPPD) solution and ferrous sulfate at a ratio of 1:25 was added to initiate reaction. Absorbance was measured by a spectrophotometer plate reader (Biotek, Synergy HT) at 505 nm. Serum levels of ROS were calculated from a calibration curve of H_2O_2 and expressed as H_2O_2 equivalent (1 unit = 1.0 mg H_2O_2/L). The calibration curve for standard solution was obtained by calculating slopes from an optical density graph.

2.6. Antioxidant assay

The total antioxidant status of the rat hippocampus was measured using the colorimetric ferric-reducing antioxidant potential (FRAP) assay (Benzie and Strain, 1996). Briefly, tissue samples were added to freshly prepared FRAP solution. The reduction of a ferric tripyridyltriazine (Fe^{3+}-TPTZ) complex to a ferrous form was monitored by measuring the absorbance at 593 nm after 15 min of incubation at 37 °C. Trolox (6-hydroxy-2,5,7,8-tetra- methyl-chloraman-2-carboxylic acid) was used as the standard (calibration curve), and the total antioxidant capacity of hippocampal samples was defined as the concentration of Trolox equivalent activity expressed as μM/mg of protein.

2.7. Lipid peroxidation assay

The thiobarbituric acid reactive-species (TBARs) assay was used to assess hippocampi products of lipid peroxidation, via malondialdehyde (MDA) (Coelho-Santos et al., 2018). Briefly, hippocampi tissue supernatant were incubated at RT in the dark for 1 h in a TBA solution together with butylhydroxytoluene (BHT; Sigma-Aldrich) and a catalyzer (Iron III chloride; Sigma-Aldrich). Afterwards, samples were incubated at 95–100 °C for 60 min followed by butanol extraction. The supernatants were read at 532 nm (Biotek, Synergy HT) and the concentration of MDA was calculated with respect to a calibration curve using 1,1,3,

3-tetramethoxypropane (Sigma-Aldrich) as the external standard (range: 0.1–83.5 μM). Results were expressed as μM/mg of hippocampi tissue concentration of lipid peroxides.

2.8. Y-maze spontaneous alternation test

The Y-maze spontaneous alternation paradigm is based on the natural tendency of rodents to explore a novel environment (Dudchenko, 2004). This test is widely used as a behavioral assay for hippocampal integrity and allows the evaluation of working memory. Selective sensitivity of spontaneous alternation to hippocampal lesions and robust age-dependency late in the postnatal period strongly support the use of this test to study hippocampal function (Albani et al., 2014).

The Y-maze apparatus consists of three arms made of black plastic (50 cm long, 20 cm high, 10 cm wide) extending from a central platform at an angle of 120°. Each mouse had free access to all three arms during 8 min. Percentage of spontaneous alternation was defined as the ratio of actual (total alternations) to possible (total arm entries-2) number of alternations × 100. Total entries were scored as an index of ambulatory activity in the Y-maze, and rats showing scores below six entries were excluded.

2.9. Brain endothelial cell cultures

Human samples were obtained from discarded temporal lobe tissue during operative treatment of epilepsy (outside epileptogenic foci) after informed consent and institutional review board ethical approval at the Neurosurgery Service, Coimbra Hospital and University Centre, Coimbra, Portugal. Primary cultures of human brain microvascular endothelial cells (HBMVECs) were isolated from microvessels obtained from the brain resection path of patients (showing no abnormalities) undergoing surgery for the treatment of intractable epilepsy, as previously described (Bernas et al., 2010; Coelho-Santos et al., 2016).

2.10. Caveolin-1 silencing

HBMVECs at about 70% confluence were transiently transfected with Cav1 specific short interfering RNA (siRNAs) (Hs CAV1 13 FlexiTube siRNA, Qiagen, Venlo, Netherlands) at a final concentration of 10 nM using ScreenFect (InCellA, Germany) diluted in Opti-MEM (1:50) according with the manufacturer's protocol. AllStars Negative Control siRNA (Qiagen) were used as controls. Cells were incubated with the transfection complexes for 48 h under normal growth conditions before use.

2.11. Horseradish peroxidase transport

HBMVECs were seeded until confluence in type I-coated collagen 12-mm transwell filters (Costar, Corning, USA) and horseradish peroxidase (HRP) transport was determined as previously described by us (Coelho-Santos et al., 2016).

2.12. Transendothelial migration of peripheral blood mononuclear cells

Approval was obtained from the Ethics Review Board for the use of peripheral blood mononuclear cells from healthy donors´buffy coats, provided by the Portuguese Blood Institute. For quantification of transmigrated cells, peripheral blood mononuclear cells (PBMCs) were labeled with calcein-AM (Molecular Probes Inc., USA) according to the manufacturer's instructions and resuspended in TEM buffer (RPMI 1640 without phenol red + 1% BSA) prior to transmigration assays. PBMCs (10^6) from the same donor suspended in TEM buffer were added to the upper side of the insert and allowed to transmigrate for 24 h. For chemokine-driven migration we used as positive control 100 ng/mL CXCL12 (SDF1-α; Proteintech Group Inc, UK) that were placed in the lower chamber. PBMCs were counted in samples obtained from the bottom chamber by measuring fluorescence at 530 nm using microplate spectroflurometer. Fluorescence values of migrated PBMCs were compared to a standard curve of known cell numbers for quantitation.

2.13. Statistical analysis

Results are expressed as mean + standard error of the mean (S.E.M.). Data were analyzed using Student's *t*-test or one-way ANOVA followed by Bonferroni's post hoc test. The level of significance was $P < 0.05$ and the "n" represents the total number of animals or the total number of experiments obtained from at least three independent cell cultures. Statistical analysis was calculated using Prism 6.0 (GraphPad Software, USA).

3. Results

3.1. MPH increases hippocampal BBB permeability by promoting vesicular transport

We recently demonstrated that acute MPH exposure causes brain endothelial hyperpermeability through caveolae-mediated transcytosis (Coelho-Santos et al., 2016), and that chronic MPH 5 exposure leads to cortical BBB dysfunction (Coelho-Santos et al., 2018). Herein, for the first time we concluded that MPH 5 is also able to promote hippocampal BBB permeability, which was shown by the presence of albumin extravasation in the hippocampal parenchyma (Fig. 1(A)) and by western blot (Fig. 1(B); $F_{(2,56)} = 3.318$, $p = 0.0435$). Albumin is a blood serum protein with high molecular weight that under normal conditions does not cross BBB. Knowing that endothelial intercellular junction seal is critical for the BBB function, we further evaluated the hippocampal protein levels of the TJ protein claudin-5 (Fig. 2(A); $F_{(2,54)} = 0.3236$, $p = 0.7249$) and the AJ protein vascular-endothelial cadherin (VE-cadherin; Fig. 2(B); $F_{(2,18)} = 0.7409$, $p = 0.4907$). No significant alterations were observed with both MPH doses. In contrast, Cav1, the major protein of caveolae vesicles, was upregulated with MPH 5 (Fig. 2(C); $F_{(2,66)} = 5076$; $p = 0.0089$) together with an increase in the number of vesicles observed by electron microscopy (Fig. 2(D); highlighted in black). In accordance

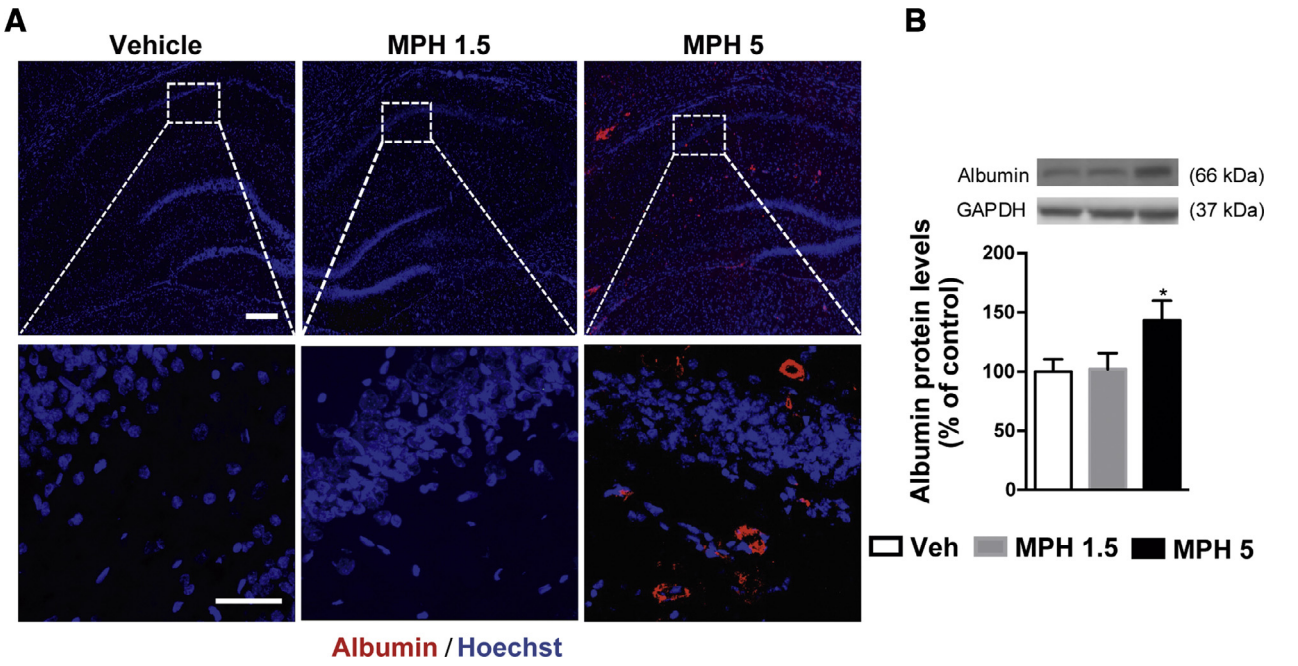

Fig. 1 Hippocampal BBB permeability triggered by MPH chronic administration. (**A**) Representative confocal images of albumin immunoreactivity (red). Hoechst 33342 (blue; nuclear marker). Scale bars: 50 and 500 μm. (B) Albumin protein levels quantification. Above the bars, representative western blot images are shown. The results are shown as mean % of control + S.E.M., $n = 6$–9 animals per condition. $^{*}P < 0.05$, using one-way ANOVA followed by Bonferroni's test. **(For interpretation of the references to color in this figure legend, the reader is referred to the web version of this article.)**

with western blot results, no changes of the intercellular junctions were identified (Fig. 2(D); arrow head), pointing to an intact paracellular pathway.

Brain ECs constitute the anatomic basis of BBB and their dysfunction will contribute to barrier disruption. To unravel cellular mechanisms that may lead to brain vascular permeability, we used freshly prepared primary human BMVECs since this *in vitro* model is clinically relevant and preserves many and important characteristics of the intact BBB (Cardoso et al., 2010; Bernas et al., 2010). Noteworthy, we have also successfully used human BMVECs in previous studies (Coelho-Santos et al., 2015; 2016). Thus, taking advantage of this *in vitro* BBB model we proved that MPH (100 μM for 24 h) increased Cav1 phosphorylation at Tyr^{14} (p-$Cav1^{y14}$, Fig. 2(E); $F_{(2,44)} = 0.2585$, $p < 0.0001$), which is necessary to caveolae-mediated endocytosis (Fernandez et al., 2002). To validate the involvement of Cav1 in MPH-induced vesicular transport of HRP, we knockdown Cav1 by transfecting endothelial cells with Cav1 siRNA (Fig. 2(F); $F_{(2,44)} = 16.60$, $P < 0.0001$). Importantly, Cav1 siRNA significantly abrogated MPH-mediated transcellular transport (Fig. 2(G); $F_{(2,28)} = 0.4675$, $p < 0.0001$). These findings uncovered the role of Cav1 in promoting MPH-induced vesicular endothelial transport.

Our data demonstrate that MPH interferes with hippocampal BBB function and directly with ECs properties by promoting vesicular transport. Moreover, we identified Cav1 signaling pathway as a key mechanism in MPH-induced transcytosis.

3.2. MPH upregulates adhesion molecules and promotes brain leukocyte infiltration

Alterations in BBB may affect its permeability and subsequently the movement of immune mediators into the brain leading to neural damage/dysfunction. ECs actively participate in leukocyte recruitment *via* the expression of inflammation-related genes, including cell adhesion molecules such as intracellular and vascular adhesion molecule-1 (ICAM-1 and VCAM-1, respectively). Thus, we hypothesized that MPH could upregulate the expression of cell adhesion molecules in ECs, and therefore promoting the infiltration of leukocytes. We concluded that MPH 5 increased the hippocampal protein levels of VCAM-1 (Fig. 3(A); $F_{(2,44)} = 4.709$, $p = 0.0140$) and ICAM-1 (Fig. 3(B); $F_{(2,28)} = 3.375$, $p = 0.0486$). Additionally, we observed the presence of $CD45^{+}$leukocytes and $CD169^{+}$ macrophages in the hippocampus of WKY rats treated with MPH 5 (Fig. 3(C)).

In accordance with animal studies we also found that MPH (100 μM, 24 h) upregulated VCAM-1 protein levels in HBMVECs. Knowing that Cav1 is involved in the regulation of endothelial permeability and leukocyte diapedesis (Choi et al., 2016; Wu et al., 2016), we further proved that Cav1 knockdown led to a decrease of VCAM-1 levels (Fig. 3(D); $F_{(3,42)} = 27.29$, $p < 0.0001$). Additionally, to unravel the involvement of Cav1 in MPH-induced diapedesis we analyzed transendothelial migration of leukocytes. Specifically, T, B, and natural killer cells, monocytes, and neutrophils-labeled with calcein-AM were added to HMBMECs in the presence or

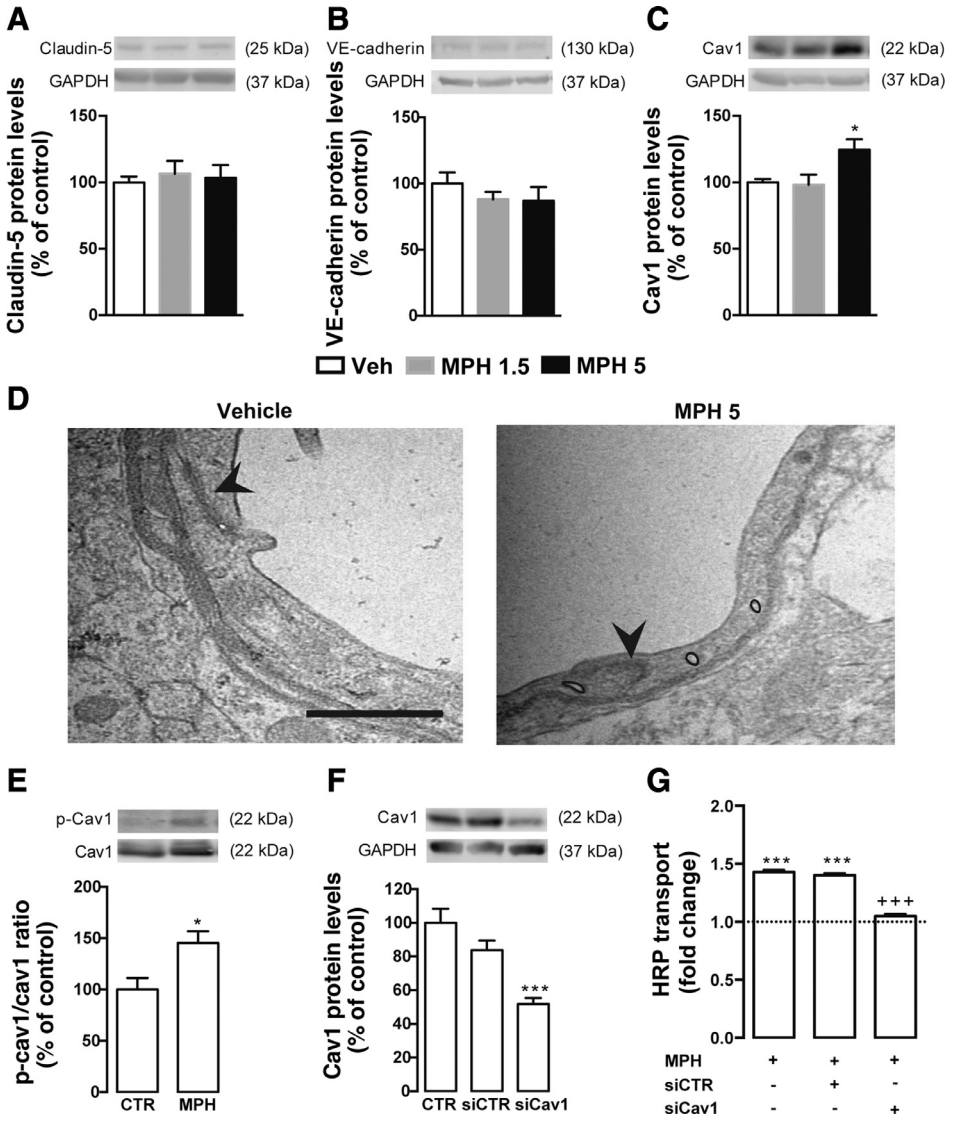

Fig. 2 MPH increases endothelial vesicular transport without affecting intercellular junctions. Protein levels of (A) claudin-5, (B) VE-cadherin and (C) caveolin-1 (Cav1). (D) Transmission electron microscopy revealed that MPH had no effect on intercellular junctions (head arrows) but triggered the formation of pinocytotic vesicles (outlined in black). Scale bar: 1 μm. (E) Cav1 Tyr14 (p-Cav1^{Y14}) phosphorylation in HBMVECs. (F) Quantification of Cav1 protein levels in HBMVECs after siRNA-mediated knockdown. Above the bars, representative western blot images are shown. (G) HRP transport in HBMVECs. The results are shown as mean + S.E.M., $n = 6$–9 animals per condition or $n = 4$ independent endothelial primary cultures. $^{*}P < 0.05$, $^{***}P < 0.001$, compared to the vehicle (Veh) or untreated cells (CTR or dashed line); $^{+++}P < 0.001$ compared to MPH, using Student's *t*-test or one-way ANOVA followed by Bonferroni's.

absence of MPH. We showed that MPH promotes the transmigration of leukocytes (Fig. 3(E)), and that Cav1 is involved in such process because the effect of MPH was abolished in the presence of siCav1 (Fig. 3(E); $F_{(4,18)} = 30.82$, $p < 0.0001$). As positive control, we used CXCL12 (SDF-1, 100 ng/mL) in the abluminal side of the transwell system. CXCL12 induced a significant increase in PBMCs transmigration across HBMECs similar to that observed in the presence of MPH (Fig. 3(E)).

We concluded that MPH promotes the infiltration of leukocytes into the brain through a caveolae-dependent transcytosis pathway.

3.3. MPH induces extracellular matrix degradation concomitantly with increased matrix metalloproteinase-9 expression and oxidative stress

The process of leukocyte transmigration involves basal lamina breaching, and collagen IV is one of the most expressed extracellular matrix protein (Zhang et al., 2013). Since we observed a transcellular migration (Fig. 3) we further investigated the effect of MPH on basal lamina. In fact, a decrease of collagen IV staining was observed with MPH 5 (Fig. 4(A) and (B)), which is coincident with

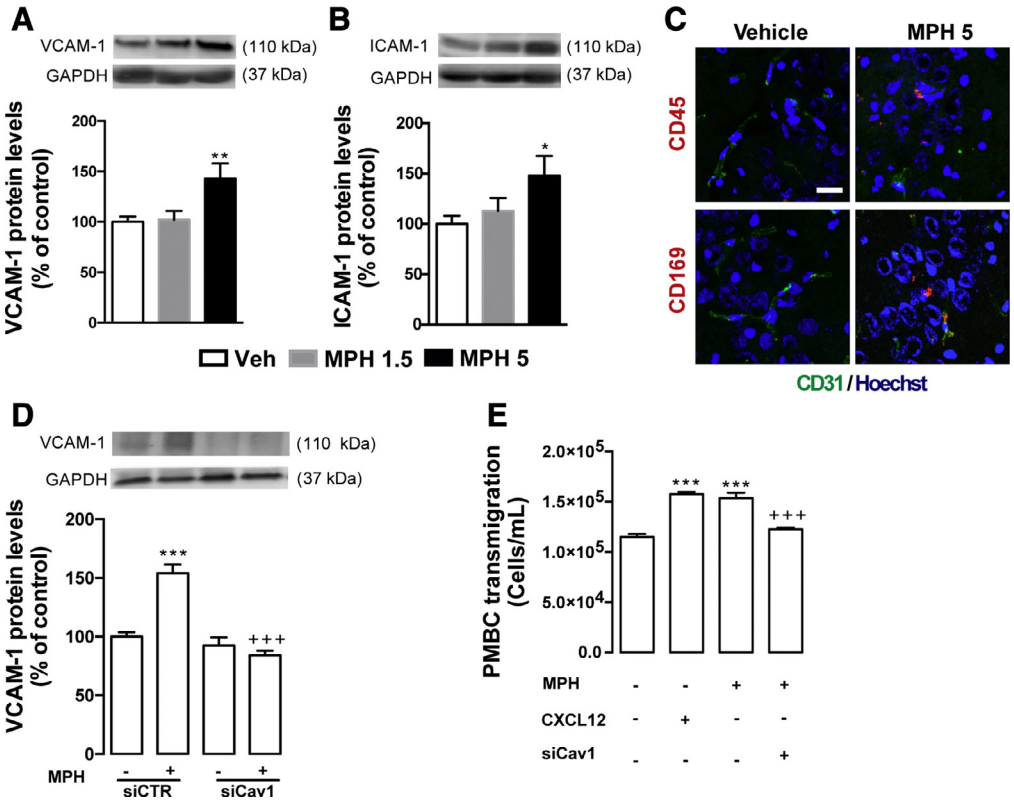

Fig. 3 Impact of MPH on brain immune quiescence. Protein levels of (**A**) vascular cell adhesion molecule-1 (VCAM-1) and (B) intercellular adhesion molecule-1 (ICAM-1) after MPH administration. (**C**) Representative images of CD31 (green; brain endothelial cells), CD45 (red; lymphocyte common antigen), and CD169 (red; Sialoadhesin, macrophage-restricted cell surface receptor). Hoechst 33342 (blue; nuclear marker). Scale bar: 20 μm. (D) Knockdown of Cav1 (siCav1) in HBMVECs prevented MPH-increased levels of VCAM-1. (E) Peripheral blood mononuclear cells (PBMC) transmigration. CXCL12 was used as positive stimulus. The results are shown as mean + S.E.M., $n = 6$-9 animals or $n = 4$ independent endothelial primary cultures. $^{*}P < 0.05$, $^{**}P < 0.01$, $^{***}P < 0.001$, compared to the vehicle (veh) or untreated cells; $^{+++}P < 0.001$ compared to MPH, using one-way ANOVA followed by Bonferroni's. **(For interpretation of the references to color in this figure legend, the reader is referred to the web version of this article.)**

the presence of albumin in the brain parenchyma (Fig. 1(A) and (B)). Additionally, leukocyte extravasation requires MMPs secretion that will degrade the extracellular matrix allowing leukocyte to penetrate through the basement membrane into the brain parenchyma. Since MMP-9 has been associated with BBB leakage via degradation of basement membrane components such as collagen IV, special attention was paid to this MMP (Asahi et al., 2001). In fact, the increase of MMP-9 immunoreactivity on the perivascular zone induced by MPH 5 was concomitant with the decrease of collagen IV (Fig. 4(C); $F_{(2,22)} = 57.49$, $p < 0.0001$). In accordance, MPH administration resulted in a significant increase of MMP-9 protein levels (Fig. 4(D); $F_{(2,44)} = 13{,}26$, $p < 0.0001$), specifically the 63-67 kDa band that correspond to the active form of MMP-9.

Oxidative stress is closely related to pathological alterations of BBB involving the activation of MMPs (Gu et al., 2002). Herein, we concluded that MPH 5 significantly increased hippocampal ROS levels (Fig. 5(A); $F_{(2,13)} = 76.78$, $p < 0.0001$). Additionally, the non-enzymatic antioxidant status (Fig. 5(B); $F_{(2,15)} = 4.305$, $p < 0.0333$) also decreased with MPH 5. MDA, the breakdown product of polyunsaturated fatty acids oxidation that is a reliable oxidant marker of oxidative stress-mediated lipid peroxidation (Uzar et al., 2006), was upregulated under the same experimental condition (Fig. 5(C); $F_{(2,13)} = 16.73$, $p < 0.0022$). Accordingly, 3-NT immunoreactivity, a maker of oxidative/nitrosative stress, was identified in cerebral microvessels (Fig. 5(D)) suggesting a perivascular production of ROS.

We showed that MPH promoted the degradation of the hippocampal basal lamina, which was concomitant with the generation of MMP-9 and an oxidative response at the perivascular zone that can explain the previously observed BBB permeability.

3.4. Morphological changes in hippocampal astrocytes triggered by MPH and astrocyte-vasculature interaction

Knowing that endothelial-astrocyte stability at the NVU requires matrix adhesion, we further investigated if MPH induced extracellular matrix degradation could affect astrocytic morphology. Hippocampal GFAP protein levels were determined and no statistical significances were observed in MPH 1.5 group (Fig. 6(A) and (B)). However, with the higher dose of MPH there was a decrease of GFAP immunoreactivity and protein levels (Fig. 6(A), B; $F_{(2,94)} = 4189$, $p = 0.0181$), as well as a significant reduction in their cytoskeletal surface area (Fig. 6(D)-(F). Looking in more detail to cell

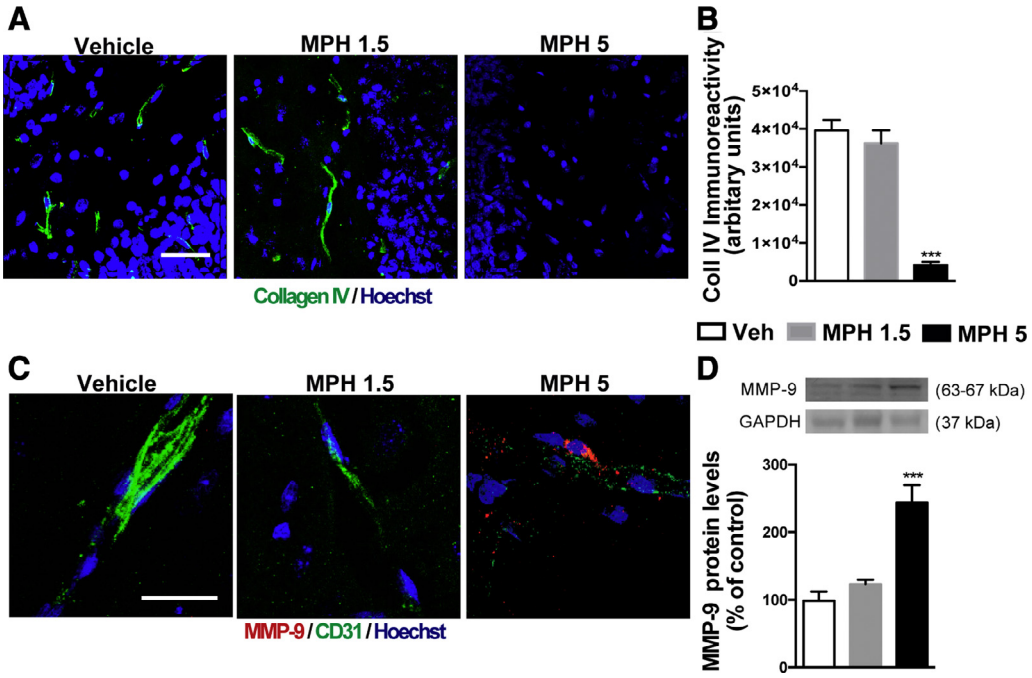

Fig. 4 MPH promotes the degradation of basal lamina concomitantly with an upregulation of MMP-9. (**A**) Collagen IV (Coll IV; green) representative images. Hoechst 33,342 (blue; nuclear marker). Scale bar: 50 μm. (B) Coll IV immunofluorescence quantification. (**C**) Representative images of matrix metalloproteinase-9 (MMP-9; red) at the perivascular zone (CD31, vessels marker; green). Hoechst 33342 (blue; nuclear marker). Scale bar: 50 μm. (D) MMP-9 protein levels. Above the bars, representative western blot images are shown. The results are shown as mean + S.E.M., $n = 6$–9 animals per condition. $^{***}P < 0.001$, using one-way ANOVA followed by Bonferroni's test. **(For interpretation of the references to color in this figure legend, the reader is referred to the web version of this article.)**

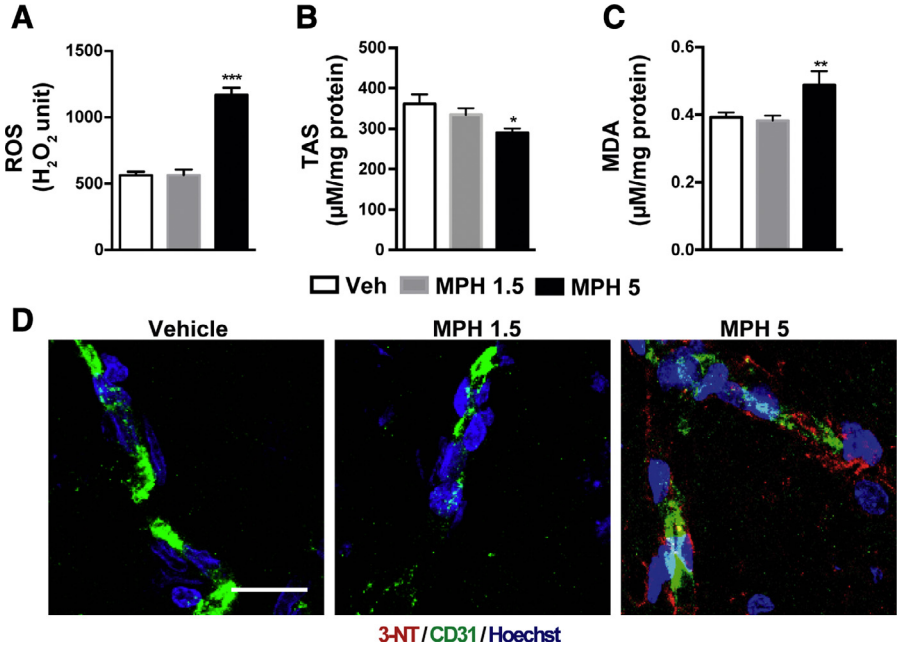

Fig. 5 MPH induces an oxidative stress response. (A) Reactive oxygen species (ROS) production, (B) non-enzymatic antioxidant activity levels (TAS) and (**C**) malondialdehyde (MDA) formation. (D) Representative images of 3-nitrotirosyne staining (3NT; red) in hippocampal microvessels stained with CD31 (green). The results are shown as mean + S.E.M., $n = 6$–9 animals per condition. $^{*}P < 0.05$, $^{**}P < 0.01$, $^{***}P < 0.001$, using one-way ANOVA followed by Bonferroni's test. **(For interpretation of the references to color in this figure legend, the reader is referred to the web version of this article.)**

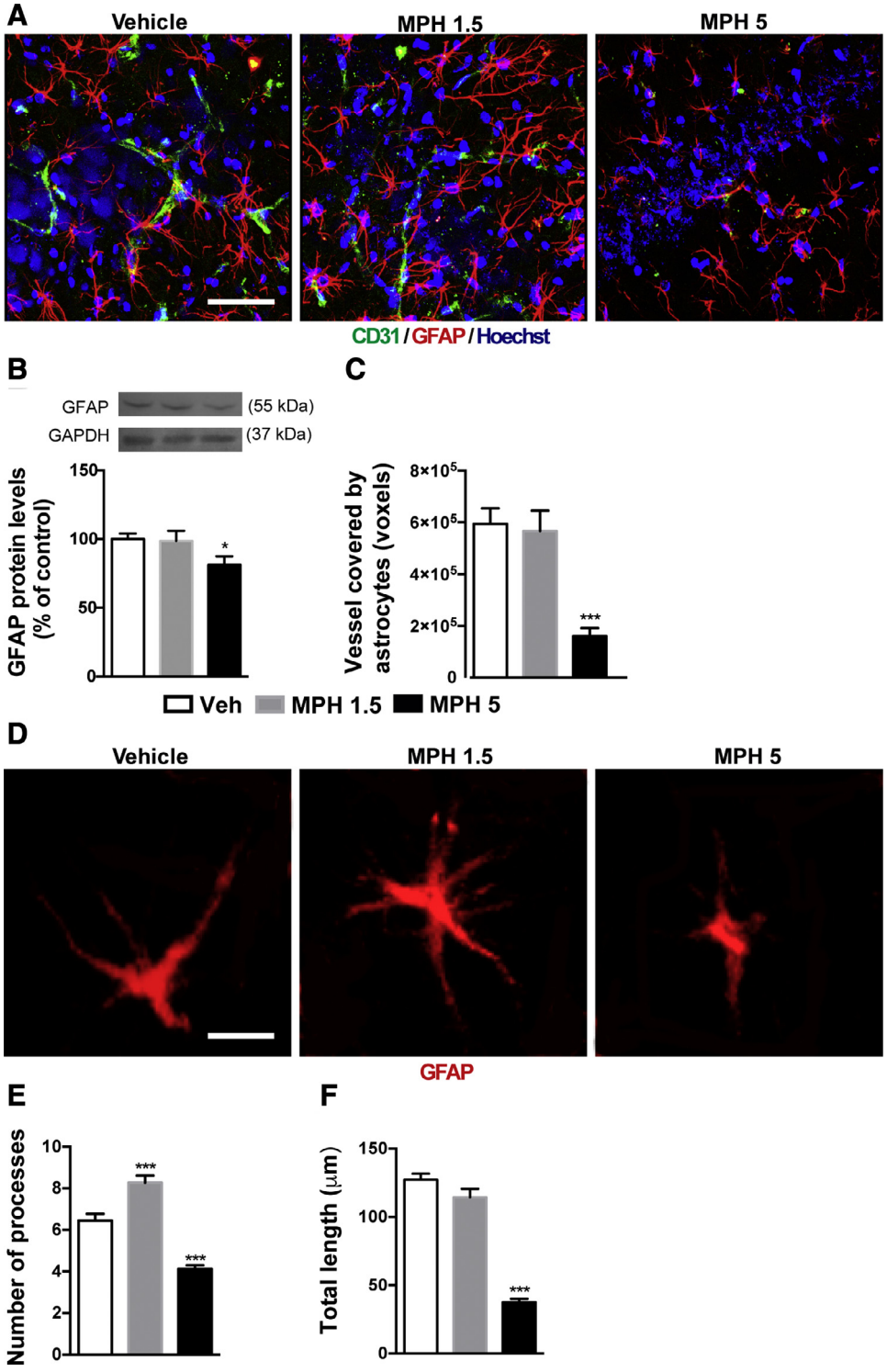

Fig. 6 MPH disrupts astrocyte-vascular coupling and causes morphological alterations in astrocytes. (**A**) Representative confocal images of microvessels (CD31; green) and astrocyte-specific GFAP antibody (red). Hoechst 33342 (blue; nuclear marker). Scale bar: 20 μm. (B) GFAP protein levels. Above the bars, representative western blot images are shown, $n = 6$-9 animals per condition. (**C**) Area fraction per field of CD31 and GFAP positive staining. (D) Representative confocal images of astrocytes (anti-GFAP). Scale bar: 20 μm. (E and F) Morphological alterations in astrocytes were analyzed in detail by the quantification of (E) total number and (F) total length of cell processes. The results are shown as mean + S.E.M., $n = 3$ animals per condition. $^{*}P < 0.05$, $^{***}P < 0.001$ using one-way ANOVA followed by Bonferroni's test. **(For interpretation of the references to color in this figure legend, the reader is referred to the web version of this article.)**

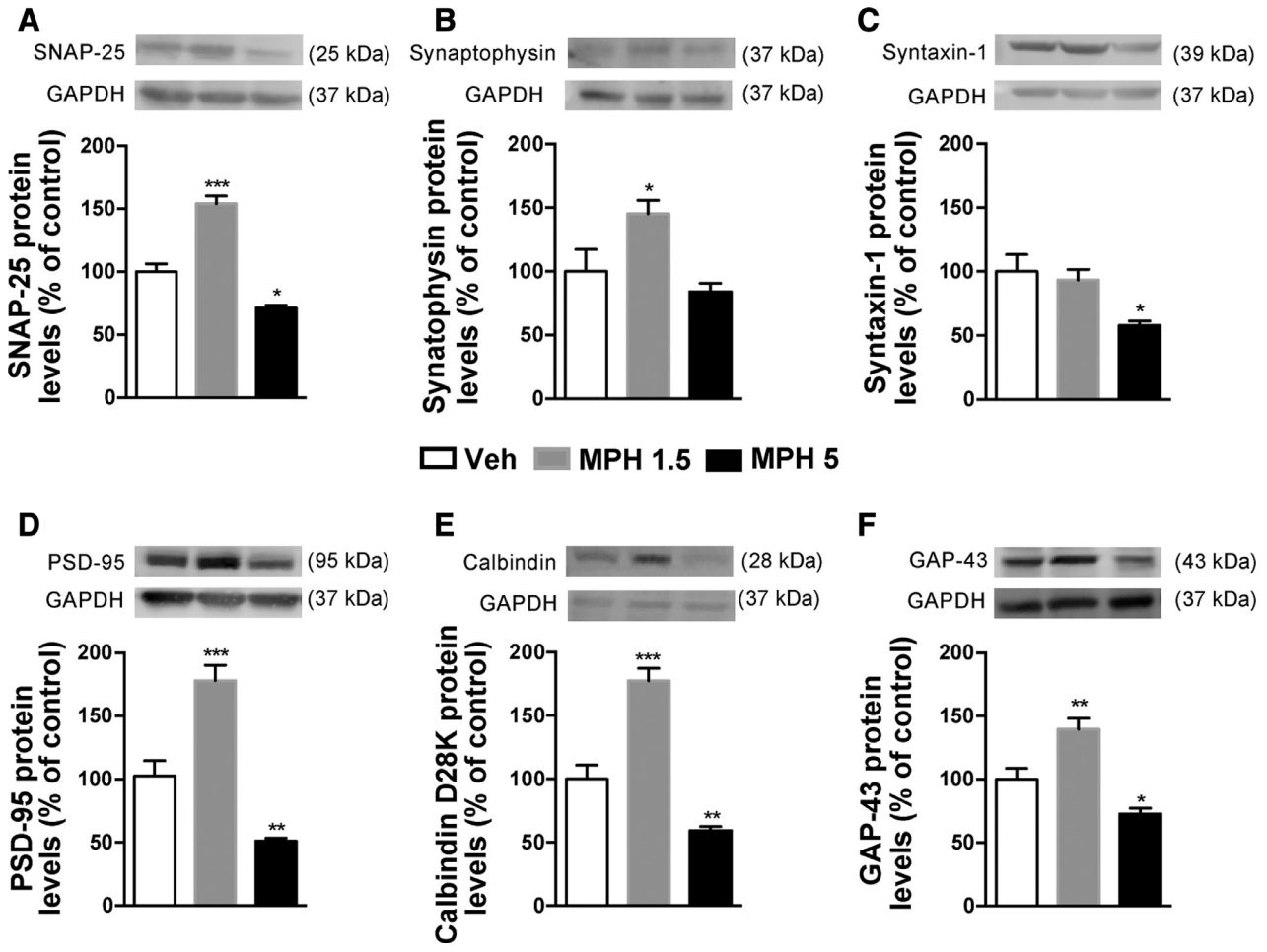

Fig. 7 MPH treatment influences the network of synaptic proteins. The protein levels of (**A**) SNAP-25, (B) synaptophysin, (C) syntaxin-1, (D) PSD-95, (E) calbindin D28K, and (F) GAP-43 were analyzed. Above the bars, representative western blot images are shown. The results are shown as mean % of control + S.E.M, $n = 6$-9 animals per condition. $^{*}P < 0.05$, $^{**}P < 0.01$, $^{***}P < 0.001$, using one-way ANOVA followed by Bonferroni's test.

morphology, we observed thinner and shorter astroglial stained processes, whereas in vehicle rats was possible to identify well-defined GFAP-positive astrocyte processes (Fig. 6(A), (D)-(F); $F_{(2,22)} = 6.75$, $p < 0.0001$). Also, the blood vessels of rats treated with MPH 5 showed less GFAP expression in the perivascular zone than vehicle rats, which was translated by the decrease of astrocytic-coverage vessels (Fig. 6(C); $F_{(2,22)} = 16.75$, $p < 0.0001$). Interestingly, MPH 1.5 increased the number of astrocytic processes although the length was not altered (Fig. 6(E) and (F)); $F_{(2,22)} = 16.75$, $p < 0.0001$).

Here, we demonstrated that a lower dose of MPH increases the number of astrocytic processes, whereas a higher dose impairs astrocytic cytoskeletal branching and decreases the vessel coverage. This is coincident with the degradation of collagen IV, the entrance of immune cells into the brain parenchyma, and in sum, with BBB hyperpermeability.

3.5. Neuronal alterations induced by MPH

To understand if astrocytic morphological alterations could reflect neuronal synaptic alterations, we evaluated the effect of on several pre- and post-synaptic proteins, namely synaptosomal-associated protein-25 (SNAP-25), synaptophysin, syntaxin-1, and postsynaptic density-95 (PSD-95). We also looked to calbindin D28k, a calcium-binding protein that plays an important role in neuronal survival, spatial learning paradigms and synaptic plasticity. Additionally, the neuronal growth-associated protein 43 kD (GAP-43; a marker for axonal sprouting) was also analyzed.

MPH 1.5 increased the protein levels of pre-synaptic proteins, SNAP-25 (Fig. 7(A); $F_{(2,46)} = 71.55$, $p < 0.0001$), synaptophysin (Fig. 7(B); $F_{(2,37)} = 12.24$, $p < 0.0001$), but with no effect on syntaxin-1 (Fig. 7(C); $F_{(2,44)} = 6.955$, $p = 0.0024$). Moreover, PSD-95 (Fig. 7(D); $F_{(2,36)} = 64.99$, $p < 0.0001$), calbindin D28K (Fig. 7(E); $F_{(2,72)} = 1.148$, $p < 0.0001$) and GAP-43 (Fig. 7(F); $F_{(2,36)} = 1.148$, $p < 0.0001$) were upregulated. On the contrary, MPH 5 chronic exposure decreased both pre-and post-synaptic proteins, as well as GAP-43 and calbindin D28k suggesting that at this dose MPH can impair neuronal communication.

In sum, a lower dose of MPH promotes the expression of synaptic proteins and proteins related with neurite outgrowth and axonal sprouting, which is coincident with increased astrocytic processes. On the contrary, a higher dose

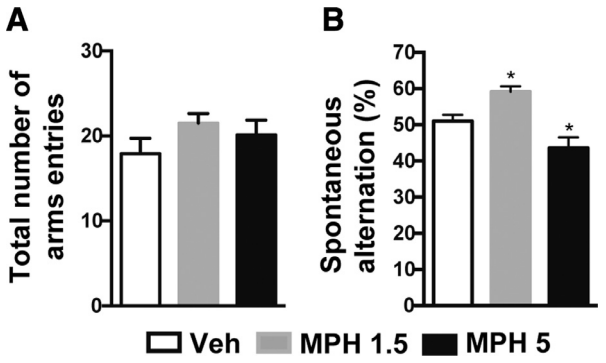

Fig. 8 Effect of MPH on spatial working memory. (**A**) The total number of arm entries. (B) Percentage of spontaneous alternations. The results are shown as mean + S.E.M, $n = 9$–13 animals of each condition. $^{*}P < 0.05$, using one-way ANOVA followed by Bonferroni's test.

of MPH leads to a down-regulation of neuronal synaptic proteins suggesting neuronal dysfunction, in parallel with astrocytic atrophy.

3.6. Impact of MPH chronic treatment on cognitive performance and signaling pathways

Brain vasculature dysfunction has been associated with cognitive performance (Gorelick et al., 2011). Thus, based on our observations regarding BBB leakage and neuronal machinery alterations, we further analyzed the rat spatial working memory (hippocampal-related behavior) by using the Y-maze test. The number of total entries were not altered by MPH (Fig. 8(A); $F_{(2,27)} = 1.148$, $p = 0.3324$). However, MPH 1.5 increased the number of spontaneous alternations (Fig. 8(B); $F_{(2,26)} = 10.40$, $p = 0.0005$), suggesting an improvement in working memory, whereas MPH 5 decreased the number of spontaneous alternations compared to vehicle (Fig. 8(B)), pointing to an impairment of cognitive performance.

To unravel the signaling pathways involved on the modulation of cognitive effects observed after MPH chronic administration, we also investigated possible alterations of key signaling proteins known to regulate both synaptic plasticity and learning/memory, such as the protein kinase B (AKT) and CREB transcription factor (Cunha et al., 2010). Rats treated with MPH 1.5 showed a significant increase in the phosphorylation of AKT (Fig. 9(A)); $F_{(2,16)} = 49.97$, $p < 0.0001$) and CREB (Fig. 9(B); $F_{(2,26)} = 80.74$, $p < 0.0001$). In accordance with the memory impairment induced by MPH 5, we observed that this dose significantly decreased phosphorylation of AKT (Fig. 9(C); $F_{(2,16)} = 49.97$, $p < 0.05$) and CREB (Fig. 9(B)); $F_{(2,26)} = 80.74$, $p < 0.01$). However, p38-mitogen-activated protein kinase (MAPK) signaling was activated, since there was an increase of p38 phosphorylation (Fig. 9(C); $F_{(2,21)} = 78.42$, $p < 0.001$).

These findings suggest that MPH induces a beneficial or detrimental effect on working memory dependent on the dose and by modulating AKT and CREB signaling pathways.

4. Discussion

Despite the widespread therapeutic use of MPH in ADHD, as well as its non-medical use (Sahakian et al., 2015), not much is known about brain alterations induced by chronic MPH consumption. Recently, we demonstrated that MPH chronic exposure leads to cortical vascular alterations particularly under physiological conditions interfering with brain immune privilege. Also, the contrasting effects on neuroimmune response observed between control and ADHD rat model support the importance of an appropriate MPH dose regimen and a more precise ADHD diagnosis (Coelho-Santos et al., 2018). Thus, we hypothesized that the long-lasting MPH exposure during development in a healthy pre-clinical model could induce hippocampal NVU alterations, which might lead to cognitive dysfunction. Overall, our results provide direct evidence that MPH 5 causes hippocampal BBB

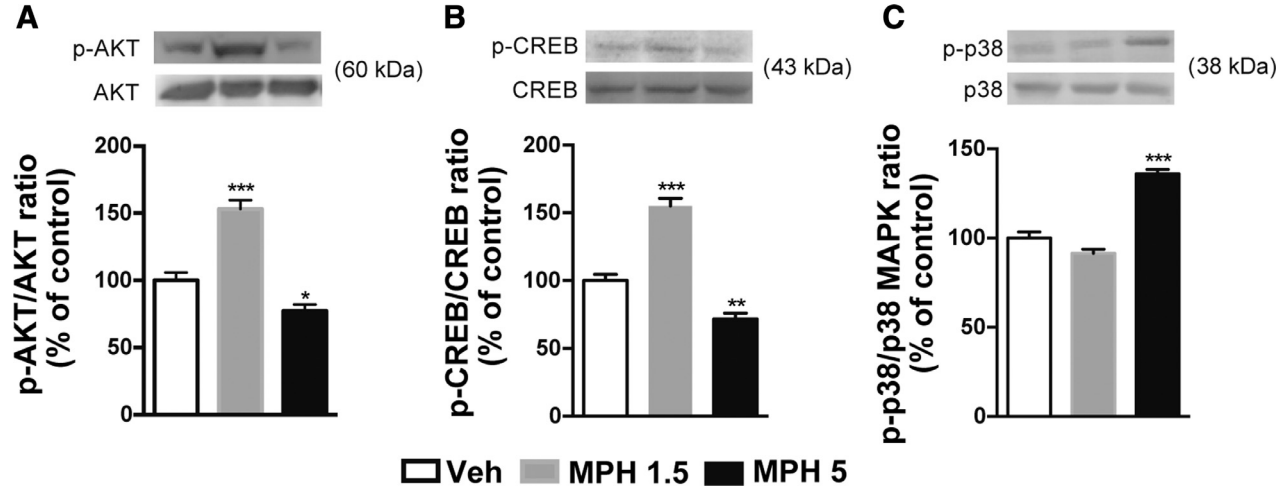

Fig. 9 MPH modulates AKT, CREB and p-38 MAPK pathways in the rat hippocampus. Phosphorylated levels of (**A**) AKT, (B) CREB and (**C**) p38 MPAK. Above the bars, representative western blot images are shown. The results are shown as mean % of control + S.E.M., $n = 6$–9 animals per condition. $^{*}P < 0.05$, $^{**}P < 0.01$, $^{***}P < 0.001$, using one-way ANOVA followed by Bonferroni's test.

disruption together with peripheral immune cells infiltration, and significant changes in both astroglial cells morphology and neuronal synaptic proteins culminating in memory impairment. On the contrary, low doses of MPH did not interfere with brain vasculature and enhanced memory probably by promoting an increase in synaptic proteins.

We have demonstrated that acute MPH exposure affects the vesicular transport across human brain ECs (Coelho-Santos et al., 2016). Since caveolae is known to be involved in the transcellular transport of albumin (Schubert et al., 2001), we now proved that the depletion of Cav1 prevented the endothelial transcytosis induced by MPH. Moreover, endothelial dysfunction was accompanied by the upregulation of adhesion molecules, VCAM-1 and ICAM-1. It is well known that adhesion molecules have a decisive role on leukocyte migration across microvasculature into brain parenchyma (Steiner et al., 2010). Noteworthy, we detected a significant increase of leukocytes in the hippocampus. By using an *in vitro* approach, we further concluded that Cav1 plays a crucial role on the transcytotic process since Cav1 knockdown decreased MPH-induced PMBCs infiltration. Thus, our findings afford a new insight for the clarification of MPH-induced caveolae endorsing hyperpermeability and provide a new perspective to design endothelial-targeted interventions to modulate vascular permeability.

The molecular framework disruption of the cerebrovascular basal lamina, which serves as the structural basis of the BBB (Gidday et al., 2005), is thought to underlie the transmigration of leukocytes. Basal membrane is mostly made of structural proteins such as collagen type IV, fibronectin and laminin, including also cell adhesion molecules and immobilized signaling proteins (Baeten and Akassoglou, 2011). Herein, we showed that MPH 5 decreased collagen IV-positive microvessels and increased MMP-9 expression. MMP-9 has been shown to be involved in the loss of BBB integrity and consequent diapedesis (Gidday et al., 2005) because many of the molecular constituents comprising the cerebrovascular basal lamina are substrates for active MMP-9 (Van den Steen et al., 2002). Besides MMP-9, it is well known that oxidative stress play a pivotal role in brain endothelium damage and so affecting BBB permeability by disrupting the paracellular and vesicular transport (Coelho-Santos et al., 2016; Haorah et al., 2007). ROS can indeed activate redox signaling pathways triggering an inflammatory response and expression of adhesion molecules in brain ECs (Kim et al., 2008). Our study shows that MPH 5 shifts the balance in favor of free-radical generation observed by increased lipid peroxidation that can cause tissue damage by react with polyunsaturated fatty acids in cellular membranes. In accordance, previous studies have documented that MPH long-term administration induces oxidative stress by decreasing the antioxidant defenses through TBARS content and protein carbonyls formation that culminates in brain cells damage in young rats (Motaghinejad et al., 2016). Moreover, we recently revealed that MPH 5 caused cortical oxidative stress (Coelho-Santos et al., 2018). Likewise, others have demonstrated that ROS promote permeability and monocyte migration across BBB, namely by activating MMPs and decreasing tissue inhibitors of MMPs (Gidday et al., 2005). The production of ROS by migrating leukocytes is thought to result from their activation following interaction with ECs (Van der Goes et al., 2001). The increase of 3-NT staining at the perivascular zone also supports the hypothesis that oxidative stress is involved in MPH-induced endothelial permeability.

The astrocytic endfeet embrace brain ECs covering almost entirely the abluminal vascular surface forming glial basal lamina, with an important role in the structure and function of cerebral endothelium (Abbott, 2002). The decrease of astrocytic vessels coverage is frequently associated with psychiatric disorders as a result of alterations in water homeostasis, blood flow, glucose transport, metabolism, and BBB function (Rajkowska et al., 2013). Here, we also observed that MPH decreased the coverage of vessels by astrocytes and downregulated GFAP expression concomitantly with BBB leakage. Since GFAP seems to play a key role in astrocytic and neuronal glutamate transporter trafficking and function (Hughes et al., 2004), changes in the distribution of this critical and normally stable protein suggest that the glutamate-glutamine cycle could be impaired by MPH. Decrease in GFAP expression has also been associated with detrimental conditions in the CNS, such as schizophrenia, bipolar disorder and depression (Johnston-Wilson et al., 2000). Moreover, low levels of GFAP make astrocytes less efficient in dealing with the acute stage of various brain injuries. (Pekny and Pekna, 2004). Actually, deficiency of glial intermediate fibers in astrocytes causes increased BBB permeability (Nico et al., 2004). With the present study we show that chronic exposure to higher doses of MPH promoted BBB dysfunction coincident with the decrease of GFAP and astrocytic vessel coverage. Additionally, we identified astrocytic atrophic with less and thinner processes when compared with the vehicle rats. This same pattern of decreased astrocytic branching was observed in Alzheimerś disease and associated with cognitive deficits (Kulijewicz-Nawrot et al., 2012). On the contrary, a lower dose of MPH increased the number of total ramifications. A recent study also demonstrated that enhanced cognitive performance is coincident with astrocytic plasticity (Brockett et al., 2015).

The disruption of vessels interaction with astrocytes can result in neuronal dysfunction whereas an increase of astrocytic processes around neurons potentiates neuronal plasticity in the hippocampus and increases cognitive function (Heller and Rusakov, 2015). In rodents, one astrocyte ensheath thousands of synapses, and structural assembly of excitatory or inhibitory synapses can be mediated by physical contact with astrocytes as well as by different astrocyte-secreted proteins that regulate presynaptic and postsynaptic differentiation (Elmariah et al., 2005). Actually, we found that MPH 1.5 increased the protein levels of PSD-95, SNAP-25, synaptophysin, GAP-43 and calbindin D28k. Synaptophysin and SNAP-25 dysfunction is linked to ADHD (Brookes et al., 2006; Brophy et al., 2002), so this increase could explain MPH effect to improve ADHD symptoms (Turner et al., 2005). Regarding calbindin D28K, this protein is downregulated in ADHD animal model, and MPH (1 mg/kg) was able to increase calbindin D28K (Yun et al., 2014). PSD-95 and GAP-43 are important to synaptic plasticity and formation of new synapses (Aigner et al., 1995; El-Husseini et al., 2000). Moreover, GAP-23 upregulation also seems to be beneficial for immune modulation and neuronal survival after CNS injury (Hung et al., 2016). This way, the increase of GAP-43 could explain the increase of astrocytic processes after a

low dose of MPH. In contrast, we found that MPH induced atrophy of astrocytes expressing less and thinner processes as well as reduced gliovascular interaction, which was coincident with a downregulation of synaptic proteins. In accordance, Lima et al. (2014) demonstrated that a reduction in the number of astrocytes alters cognitive performance. Based on these results, we can suggest that higher doses of MPH compromise neuronal events impairing functional connectivity. It was already shown that MPH chronic treatment causes a loss of neurons in the rat hippocampus (Schmitz et al., 2016). Additionally, early chronic administration of 5 mg/kg (daily for 21 days) induced hippocampal shape deformations and affected topological features of ventral hippocampal functional networks (van der Marel et al., 2015).

In the past two decades there was an increase non-medical use of MPH for cognitive enhancement in healthy individuals (McCabe et al., 2014). Herein, besides cellular alterations triggered by MPH in the hippocampus, we also aimed to understand the effects of chronic consumption of this psychostimulant on memory. It is well established the involvement of hippocampus in learning and memory processes (Bird and Burgess, 2008). Thus, we focus our work on working memory, which is generally defined as cognitive entities related to temporary storage and operation of information. Moreover, MPH is known to modulate neurotransmission interfering with executive functions and working memory in healthy individuals (Repantis et al., 2010). Likewise, MPH treatment seems to potentiate synaptic plasticity, in age-dependent manner. Potential benefits and risks of cognitive enhancement highly depends on drug dose and task requirements. Pre-clinical studies showed that acute administration of 5 mg/kg MPH improved whereas 50 mg/kg disrupted recognition memory (Mioranzza et al., 2011). Furthermore, rats administered with MPH (2 mg/kg/day) presented an upregulation of striatal genes involved in synaptic plasticity, namely the formation, maturation, and stabilization of new neural connections (Adriani et al., 2006). Also, the administration of MPH to those with "normal" catecholamine function alters cognitive function, with low doses enhancing performance and higher doses increasing catecholamine levels above optimal values leading to glutamate receptors blockade and consequently to neuronal network impairment (Cheng et al., 2014). Additionally, several observations converged on the conclusion that the dose-response curve has an asymptotic U shape, such that there are diminishing therapeutic gains at progressively higher doses of MPH (Devilbiss and Berridge, 2008).

In this study, we observed that MPH 1.5 increased short-term memory performance and activated AKT/CREB cascade. Accordingly, Andersen et al. (2002) demonstrated that treatment with a similar dose of MPH (2.0 mg/kg) during the same developmental period caused a sustained increase in CREB levels in the nucleus accumbens. On the contrary, a higher dose of MPH caused NVU dysfunction and downregulated AKT/CREB pathways, but induced the activation of p38 MAPK. Noteworthy, it was already demonstrated that BBB opening and subsequent infiltration of serum components into brain parenchyma triggers a sequence of processes that lead to neuronal dysfunction, which can culminate in cognitive impairment (Serlin et al., 2011). Moreover, at this same dose of MPH an increase of ROS was found in the hippocampus, namely at the perivascular zone. ROS may act as second messengers arbitrating the cellular pathways (Zhang et al., 2016), which can explain the inhibition of AKT/CREB. Noteworthy, ROS also induce the activation of p38-MAPK signaling that is involved in long-term depression, a persistent activity-dependent decrease of synaptic efficacy (Huang et al., 2004). In addition, lipid peroxidation affects the membrane biophysical properties and integrity that leads to impairments in long-term potentiation (Ojo et al., 2015). The synaptic modulation and memory effects triggered by chronic MPH treatment in the present study are consistent with the hypothesis that psychostimulants produce a persistent reorganization of patterns of synaptic connectivity in brain regions including the hippocampus, which may impair cognitive behavior in "normal" rats (Robinson and Kolb, 2004).

In conclusion, the present study reveals that low doses of MPH in normal rats improves memory performance associated with modulation of astrocytic morphology and synaptic machinery. However, higher doses of MPH lead to hippocampal NVU alterations and memory impairment. The present findings emphasize the dose-dependent effect of chronic MPH use under non-pathological conditions.

Role of funding source

This work was supported by Project PTDC/NEU-OSD/0312/2012 from Foundation for Science and Technology (FCT Portugal) co-financed by COMPETE and FEDER funds, Pest-C/SAU/UI3282/2013-2014 and CNC.IBILI UID/NEU/04539/2013 (FEDER-COMPETE, FCOMP-01-0124-FEDER-028417 and POCI-01-0145-FEDER-007440). Also, PhD fellowships SFRH/BD/77314/2011, SFRH/BD/84408/2012 and SFRH/BD/85556/2012 from FCT Portugal co-financed by QREN and POPH/FSE.

Contributors

VCS and APS designed the study and wrote the paper. VCS, FLP, AM, MFT, RAL were involved in data acquisition. MR and MB provided the human samples. CG and CAFR contributed to the discussion. All authors have approved the manuscript.

Conflict of interest

The authors declare no conflict of interest.

Acknowledgments

We acknowledge the High Resolution Bioimaging Laboratory of the Faculty of Medicine of the University of Coimbra.

Supplementary material

Supplementary material associated with this article can be found, in the online version, at doi:10.1016/j.euroneuro.2018.12.007.

References

Abbott, N.J., 2002. Astrocyte-endothelial interactions and blood--brain barrier permeability. J. Anat. 200, 629–638.

Adriani, W., Leo, D., Guarino, M., Natoli, A., Di Consiglio, E., De Angelis, G., Traina, E., Testai, E., Perrone-Capano, C., Laviola, G., 2006. Short-term effects of adolescent methylphenidate exposure on brain striatal gene expression and sexual/endocrine parameters in male rats. Ann. N.Y. Acad. Sci. 1074, 52–73.

Aigner, L., Arber, S., Kapfhammer, J.P., Laux, T., Schneider, C., Botteri, F., Brenner, H.R., Caroni, P., 1995. Overexpression of the neural growth-associated protein GAP-43 induces nerve sprouting in the adult nervous system of transgenic mice. Cell 83, 269–278.

Albani, S.H., McHail, D.G., Dumas, T.C., 2014. Developmental studies of the hippocampus and hippocampal-dependent behaviors: insights from interdisciplinary studies and tips for new investigators. Neurosci. Biobehav. Rev. 43, 183–190.

Andersen, S.L., Arvanitogiannis, A., Pliakas, A.M., LeBlanc, C., Carlezon Jr., W.A., 2002. Altered responsiveness to cocaine in rats exposed to methylphenidate during development. Nat. Neurosci. 5, 13–14.

Asahi, M., Wang, X., Mori, T., Sumii, T., Jung, J.C., Moskowitz, M.A., Fini, M.E., Lo, E.H., 2001. Effects of matrix metalloproteinase-9 gene knock-out on the proteolysis of blood-brain barrier and white matter components after cerebral ischemia. J. Neurosci. 21, 7724–7732.

Baeten, K.M., Akassoglou, K., 2011. Extracellular matrix and matrix receptors in blood-brain barrier formation and stroke. Dev. Neurobiol. 71, 1018–1039.

Bahcelioglu, M., Gozil, R., Take, G., Elmas, C., Oktem, H., Kadioglu, D., Calguner, E., Erdogan, D., Sargon, M.F., Yazici, A.C., Tas, M., Bardakci, Y., Senol, S., 2009. Dose-related immunohistochemical and ultrastructural changes after oral methylphenidate administration in cerebrum and cerebellum of the rat. World J. Biol. Psychiatry 10, 531–543. doi:10.1080/15622970903176683.

Benzie, I.F., Strain, J.J., 1996. The ferric reducing ability of plasma (FRAP) as a measure of "antioxidant power": the FRAP assay. Anal. Biochem. 239, 70–76.

Bernas, M.J., Cardoso, F.L., Daley, S.K., Weinand, M.E., Campos, A.R., Ferreira, A.J., Hoying, J.B., Witte, M.H., Brites, D., Persidsky, Y., Ramirez, S.H., Brito, M.A., 2010. Establishment of primary cultures of human brain microvascular endothelial cells to provide an *in vitro* cellular model of the blood-brain barrier. Nat. Protoc. 5, 1265–1272.

Bird, C.M., Burgess, N., 2008. The hippocampus and memory: insights from spatial processing. Nat. Rev. Neurosci. 9, 182–194.

Brockett, A.T., LaMarca, E.A., Gould, E., 2015. Physical exercise enhances cognitive flexibility as well as astrocytic and synaptic markers in the medial prefrontal cortex. PLoS One 10, e0124859. doi:10.1371/journal.pone.0124859.

Brookes, K., Xu, X., Chen, W., Zhou, K., Neale, B., Lowe, N., Anney, R., Franke, B., Gill, M., Ebstein, R., Buitelaar, J., Sham, P., Campbell, D., Knight, J., Andreou, P., Altink, M., Arnold, R., Boer, F., Buschgens, C., Butler, L., Christiansen, H., Feldman, L., Fleischman, K., Fliers, E., Howe-Forbes, R., Goldfarb, A., Heise, A., Gabriels, I., Korn-Lubetzki, I., Johansson, L., Marco, R., Medad, S., Minderaa, R., Mulas, F., Muller, U., Mulligan, A., Rabin, K., Rommelse, N., Sethna, V., Sorohan, J., Uebel, H., Psychogiou, L., Weeks, A., Barrett, R., Craig, I., Banaschewski, T., Sonuga-Barke, E., Eisenberg, J., Kuntsi, J., Manor, I., McGuffin, P., Miranda, A., Oades, R.D., Plomin, R., Roeyers, H., Rothenberger, A., Sergeant, J., Steinhausen, H.C., Taylor, E., Thompson, M., Faraone, S.V., Asherson, P., 2006. The analysis of 51 genes in DSM-IV combined type attention deficit hyperactivity disorder: association signals in DRD4, DAT1 and 16 other genes. Mol. Psychiatry 11, 934–953.

Brophy, K., Hawi, Z., Kirley, A., Fitzgerald, M., Gill, M., 2002. Synaptosomal-associated protein 25 (SNAP-25) and attention deficit hyperactivity disorder (ADHD): evidence of linkage and association in the Irish population. Mol. Psychiatry 7, 913–917.

Cardoso, F.L., Brites, D., Brito, M.A., 2010. Looking at the blood--brain barrier: molecular anatomy and possible investigation approaches. Brain Res. Rev. 64, 328–363.

Cecchelli, R., Berezowski, V., Lundquist, S., Culot, M., Renftel, M., Dehouck, M.P., Fenart, L., 2007. Modelling of the blood-brain barrier in drug discovery and development. Nat. Rev. Drug Discov. 6, 650–661.

Cheng, J., Xiong, Z., Duffney, L.J., Wei, J., Liu, A., Liu, S., Chen, G.J., Yan, Z., 2014. Methylphenidate exerts dose-dependent effects on glutamate receptors and behaviors. Biol. Psychiatry 76, 953–962.

Choi, K.H., Kim, H.S., Park, M.S., Kim, J.T., Kim, J.H., Cho, K.A., Lee, M.C., Lee, H.J., Cho, K.H., 2016. Regulation of Caveolin-1 expression determines early brain edema after experimental focal cerebral ischemia. Stroke 47, 1336–1343.

Coelho-Santos, V., Leitão, R.A., Cardoso, F.L., Palmela, I., Rito, M., Barbosa, M., Brito, M.A., Fontes-Ribeiro, C.A., Silva, A.P., 2015. The TNF-α/NF-κB signaling pathway has a key role in methamphetamine-induced blood-brain barrier dysfunction. J. Cereb. Blood Flow Metab. 35, 1260–1271.

Coelho-Santos, V., Socodato, R., Portugal, C., Leitão, R.A., Rito, M., Barbosa, M., Couraud, P.O., Romero, I.A., Weksler, B., Minshall, R.D., Fontes-Ribeiro, C., Summavielle, T., Relvas, J.B., Silva, A.P., 2016. Methylphenidate-triggered ROS generation promotes caveolae-mediated transcytosis via Rac1 signaling and c-Src-dependent caveolin-1 phosphorylation in human brain endothelial cells. Cell Mol. Life Sci. 73, 4701–4716.

Coelho-Santos, V., Cardoso, F.L., Leitão, R.A., Fontes-Ribeiro, C.A., Silva, A.P., 2018. Impact of developmental exposure to methylphenidate on rat brain's immune privilege and behavior: control *versus* ADHD model. Brain Behav. Immun. 68, 169–182.

Cunha, C., Brambilla, R., Thomas, K.L., 2010. A simple role for BDNF in learning and memory? Front. Mol. Neurosci. 3, 1. doi:10.3389/neuro.02.001.2010.

Devilbiss, D.M., Berridge, C.W., 2008. Cognition-enhancing doses of methylphenidate preferentially increase prefrontal cortex neuronal responsiveness. Biol. Psychiatry 64, 626–635.

Dietrich, J.B., 2009. Alteration of blood-brain barrier function by methamphetamine and cocaine. Cell Tissue Res. 336, 385–392.

Dudchenko, P.A., 2004. An overview of the tasks used to test working memory in rodents. Neurosci. Biobehav. Rev. 28, 699–709.

El-Husseini, A.E., Schnell, E., Chetkovich, D.M., Nicoll, R.A., Bredt, D.S., 2000. PSD-95 involvement in maturation of excitatory synapses. Science 290, 1364–1368.

Elmariah, S.B., Oh, E.J., Hughes, E.G., Balice-Gordon, R.J., 2005. Astrocytes regulate inhibitory synapse formation via Trk-mediated modulation of postsynaptic GABAA receptors. J. Neurosci. 25, 3638–3650.

Fernandez, I., Ying, Y., Albanesi, J., Anderson, R.G., 2002. Mechanism of caveolin filament assembly. Proc. Natl. Acad. Sci. U. S. A. 99, 11193–11198.

Gerasimov, M.R., Franceschi, M., Volkow, N.D., Gifford, A., Gatley, S.J., Marsteller, D., Molina, P.E., Dewey, S.L., 2000. Comparison between intraperitoneal and oral methylphenidate administration: a microdialysis and locomotor activity study. J. Pharmacol. Exp. Ther. 295, 51–57.

Gidday, J.M., Gasche, Y.G., Copin, J.C., Shah, A.R., Perez, R.S., Shapiro, S.D., Chan, P.H., Park, T.S., 2005. Leukocyte-derived matrix metalloproteinase-9 mediates blood-brain barrier breakdown and is proinflammatory after transient focal cerebral ischemia. Am. J. Physiol. Heart Circ. Physiol. 289, H558–H568.

Gonçalves, J., Leitão, R.A., Higuera-Matas, A., Assis, M.A., Coria, S.M., Fontes-Ribeiro, C., Ambrosio, E., Silva, A.P., 2017.

Extended-access methamphetamine self-administration elicits neuroinflammatory response along with blood-brain barrier breakdown. Brain Behav. Immun. 62, 306–317.

Gorelick, P.B., Scuteri, A., Black, S.E., Decarli, C., Greenberg, S.M., Iadecola, C., Launer, L.J., Laurent, S., Lopez, O.L., Nyenhuis, D., Petersen, R.C., Schneider, J.A., Tzourio, C., Arnett, D.K., Bennett, D.A., Chui, H.C., Higashida, R.T., Lindquist, R., Nilsson, P.M., Roman, G.C., Sellke, F.W., Seshadri, S.American Heart Association Stroke Council, C.o.E., Prevention, C.o.C.N.C.o.C.R., Intervention, Council on Cardiovascular, S., Anesthesia, 2011. Vascular contributions to cognitive impairment and dementia: a statement for healthcare professionals from the american heart association/american stroke association. Stroke 42, 2672–2713.

Gu, Z., Kaul, M., Yan, B., Kridel, S.J., Cui, J., Strongin, A., Smith, J.W., Liddington, R.C., Lipton, S.A., 2002. S-nitrosylation of matrix metalloproteinases: signaling pathway to neuronal cell death. Science 297, 1186–1190.

Haorah, J., Ramirez, S.H., Schall, K., Smith, D., Pandya, R., Persidsky, Y., 2007. Oxidative stress activates protein tyrosine kinase and matrix metalloproteinases leading to blood-brain barrier dysfunction. J. Neurochem. 101, 566–576.

Harvey, R.C., Sen, S., Deaciuc, A., Dwoskin, L.P., Kantak, K.M., 2011. Methylphenidate treatment in adolescent rats with an attention deficit/hyperactivity disorder phenotype: cocaine addiction vulnerability and dopamine transporter function. Neuropsychopharmacology 36, 837–847.

Heller, J.P., Rusakov, D.A., 2015. Morphological plasticity of astroglia: understanding synaptic microenvironment. Glia 63, 2133–2151.

Huang, C.C., You, J.L., Wu, M.Y., Hsu, K.S., 2004. Rap1-induced p38 mitogen-activated protein kinase activation facilitates AMPA receptor trafficking via the GDI.Rab5 complex. Potential role in (S)-3,5-dihydroxyphenylglycene-induced long term depression. J. Biol. Chem. 279, 12286–12292.

Hughes, E.G., Maguire, J.L., McMinn, M.T., Scholz, R.E., Sutherland, M.L., 2004. Loss of glial fibrillary acidic protein results in decreased glutamate transport and inhibition of PKA-induced EAAT2 cell surface trafficking. Brain Res. Mol. Brain Res. 124, 114–123.

Hung, C.C., Lin, C.H., Chang, H., Wang, C.Y., Lin, S.H., Hsu, P.C., Sun, Y.Y., Lin, T.N., Shie, F.S., Kao, L.S., Chou, C.M., Lee, Y.H., 2016. Astrocytic GAP43 induced by the TLR4/NF-kappaB/STAT3 axis attenuates astrogliosis-mediated microglial activation and neurotoxicity. J. Neurosci. 36, 2027–2043 1.

Johnston-Wilson, N.L., Sims, C.D., Hofmann, J.P., Anderson, L., Shore, A.D., Torrey, E.F., Yolken, R.H., 2000. Disease-specific alterations in frontal cortex brain proteins in schizophrenia, bipolar disorder, and major depressive disorder. The stanley neuropathology consortium. Mol. Psychiatry 5, 142–149.

Kim, S.R., Bae, Y.H., Bae, S.K., Choi, K.S., Yoon, K.H., Koo, T.H., Jang, H.O., Yun, I., Kim, K.W., Kwon, Y.G., Yoo, M.A., Bae, M.K., 2008. Visfatin enhances ICAM-1 and VCAM-1 expression through ROS-dependent NF-kappaB activation in endothelial cells. Biochim. Biophys. Acta 1783, 886–895.

Kousik, S.M., Napier, T.C., Carvey, P.M., 2012. The effects of psychostimulant drugs on blood brain barrier function and neuroinflammation. Front. Pharmacol. 3, 121. doi:10.3389/fphar.2012.00121.

Kulijewicz-Nawrot, M., Verkhratsky, A., Chvatal, A., Sykova, E., Rodriguez, J.J., 2012. Astrocytic cytoskeletal atrophy in the medial prefrontal cortex of a triple transgenic mouse model of Alzheimer's disease. J. Anat. 221, 252–262.

Leitão, R.A., Sereno, J., Castelhano, J.M., Goncalves, S.I., Coelho-Santos, V., Fontes-Ribeiro, C., Castelo-Branco, M., Silva, A.P., 2018. Aquaporin-4 as a new target against methamphetamine-induced brain alterations: focus on the neuroglio-vascular unit and motivational behavior. Mol. Neurobiol. 55, 2056–2069.

Lima, A., Sardinha, V.M., Oliveira, A.F., Reis, M., Mota, C., Silva, M.A., Marques, F., Cerqueira, J.J., Pinto, L., Sousa, N., Oliveira, J.F., 2014. Astrocyte pathology in the prefrontal cortex impairs the cognitive function of rats. Mol. Psychiatry 19, 834–841.

Marco, E.M., Adriani, W., Ruocco, L.A., Canese, R., Sadile, A.G., Laviola, G., 2011. Neurobehavioral adaptations to methylphenidate: the issue of early adolescent exposure. Neurosci. Biobehav. Rev. 35, 1722–1739.

Marquand, A.F., O'Daly, O.G., De Simoni, S., Alsop, D.C., Maguire, R.P., Williams, S.C., Zelaya, F.O., Mehta, M.A., 2012. Dissociable effects of methylphenidate, atomoxetine and placebo on regional cerebral blood flow in healthy volunteers at rest: a multi-class pattern recognition approach. Neuroimage 60, 1015–1024.

Martins, T., Baptista, S., Gonçalves, J., Leal, E., Milhazes, N., Borges, F., Ribeiro, C.F., Quintela, O., Lendoiro, E., Lopez-Rivadulla, M., Ambrósio, A.F., Silva, A.P., 2011. Methamphetamine transiently increases the blood-brain barrier permeability in the hippocampus: role of tight junction proteins and matrix metalloproteinase-9. Brain Res. 1411, 28–40.

McCabe, S.E., West, B.T., Teter, C.J., Boyd, C.J., 2014. Trends in medical use, diversion, and nonmedical use of prescription medications among college students from 2003 to 2013: connecting the dots. Addict. Behav. 39, 1176–1182.

Mioranzza, S., Costa, M.S., Botton, P.H., Ardais, A.P., Matte, V.L., Espinosa, J., Souza, D.O., Porciuncula, L.O., 2011. Blockade of adenosine A(1) receptors prevents methylphenidate-induced impairment of object recognition task in adult mice. Prog. Neuropsychopharmacol. Biol. Psychiatry 35, 169–176.

Motaghinejad, M., Motevalian, M., Shabab, B., 2016. Effects of chronic treatment with methylphenidate on oxidative stress and inflammation in hippocampus of adult rats. Neurosci. Lett. 619, 106–113.

Nico, B., Paola Nicchia, G., Frigeri, A., Corsi, P., Mangieri, D., Ribatti, D., Svelto, M., Roncali, L., 2004. Altered blood-brain barrier development in dystrophic MDX mice. Neuroscience 125, 921–935.

Ojo, J.O., Rezaie, P., Gabbott, P.L., Stewart, M.G., 2015. Impact of age-related neuroglial cell responses on hippocampal deterioration. Front. Aging Neurosci. 7, 57. doi:10.3389/fnagi.2015.00057.

Pekny, M., Pekna, M., 2004. Astrocyte intermediate filaments in CNS pathologies and regeneration. J. Pathol. 204, 428–437.

Rajkowska, G., Hughes, J., Stockmeier, C.A., Javier Miguel-Hidalgo, J., Maciag, D., 2013. Coverage of blood vessels by astrocytic endfeet is reduced in major depressive disorder. Biol. Psychiatry 73, 613–621.

Repantis, D., Schlattmann, P., Laisney, O., Heuser, I., 2010. Modafinil and methylphenidate for neuroenhancement in healthy individuals: a systematic review. Pharmacol. Res. 62, 187–206.

Robinson, T.E., Kolb, B., 2004. Structural plasticity associated with exposure to drugs of abuse. Neuropharmacology 47 (Suppl 1), 33–46. doi:10.1016/j.neuropharm.2004.06.025.

Sahakian, B.J., Bruhl, A.B., Cook, J., Killikelly, C., Savulich, G., Piercy, T., Hafizi, S., Perez, J., Fernandez-Egea, E., Suckling, J., Jones, P.B., 2015. The impact of neuroscience on society: cognitive enhancement in neuropsychiatric disorders and in healthy people. Philos. Trans. R. Soc. Lond. B Biol. Sci. 370, 20140214. doi:10.1098/rstb.2014.0214.

Sajja, R.K., Rahman, S., Cucullo, L., 2016. Drugs of abuse and blood-brain barrier endothelial dysfunction: a focus on the role of oxidative stress. J. Cereb. Blood Flow Metab. 36, 539–554.

Schmitz, F., Pierozan, P., Rodrigues, A.F., Biasibetti, H., Grunevald, M., Pettenuzzo, L.F., Scaini, G., Streck, E.L., Netto, C.A., Wyse, A.T., 2016. Methylphenidate causes behavioral impairments and neuron and astrocyte loss in the hippocampus of juvenile rats. Mol. Neurobiol. doi:10.1007/s12035-016-9987-y.

Schubert, W., Frank, P.G., Razani, B., Park, D.S., Chow, C.W., Lisanti, M.P., 2001. Caveolae-deficient endothelial cells show defects in the uptake and transport of albumin *in vivo*. J. Biol. Chem. 276, 48619–48622.

Serlin, Y., Levy, J., Shalev, H., 2011. Vascular pathology and blood--brain barrier disruption in cognitive and psychiatric complications of type 2 diabetes mellitus. Cardiovasc. Psychiatry Neurol. 2011, 609202.

Sharma, A., Couture, J., 2014. A review of the pathophysiology, etiology, and treatment of attention-deficit hyperactivity disorder (ADHD). Ann. Pharmacother. 48, 209–225.

Somkuwar, S.S., Darna, M., Kantak, K.M., Dwoskin, L.P., 2013. Adolescence methylphenidate treatment in a rodent model of attention deficit/hyperactivity disorder: dopamine transporter function and cellular distribution in adulthood. Biochem. Pharmacol. 86, 309–316.

Steiner, O., Coisne, C., Cecchelli, R., Boscacci, R., Deutsch, U., Engelhardt, B., Lyck, R., 2010. Differential roles for endothelial ICAM-1, ICAM-2, and VCAM-1 in shear-resistant T cell arrest, polarization, and directed crawling on blood-brain barrier endothelium. J. Immunol. 185, 4846-4855.

Swanson, J.M., Volkow, N.D., 2002. Pharmacokinetic and pharmacodynamic properties of stimulants: implications for the design of new treatments for ADHD. Behav. Brain Res. 130, 73-78.

Turner, D.C., Blackwell, A.D., Dowson, J.H., McLean, A., Sahakian, B.J., 2005. Neurocognitive effects of methylphenidate in adult attention-deficit/hyperactivity disorder. Psychopharmacology 178, 286–295 (Berl).

Urban, K.R., Gao, W.J., 2014. Performance enhancement at the cost of potential brain plasticity: neural ramifications of nootropic drugs in the healthy developing brain. Front. Syst. Neurosci. 8, 38. doi:10.3389/fnsys.2014.00038.

Uzar, E., Koyuncuoglu, H.R., Uz, E., Yilmaz, H.R., Kutluhan, S., Kilbas, S., Gultekin, F., 2006. The activities of antioxidant enzymes and the level of malondialdehyde in cerebellum of rats subjected to methotrexate: protective effect of caffeic acid phenethyl ester. Mol. Cell Biochem. 291, 63–68.

Van den Steen, P.E., Dubois, B., Nelissen, I., Rudd, P.M., Dwek, R.A., Opdenakker, G., 2002. Biochemistry and molecular biology of gelatinase B or matrix metalloproteinase-9 (MMP-9). Crit. Rev. Biochem. Mol. Biol. 37, 375–536.

Van der Goes, A., Wouters, D., Van Der Pol, S.M., Huizinga, R., Ronken, E., Adamson, P., Greenwood, J., Dijkstra, C.D., De Vries, H.E., 2001. Reactive oxygen species enhance the migration of monocytes across the blood-brain barrier *in vitro*. FASEB J. 15, 1852–1854.

van der Marel, K., Bouet, V., Meerhoff, G.F., Freret, T., Boulouard, M., Dauphin, F., Klomp, A., Lucassen, P.J., Homberg, J.R., Dijkhuizen, R.M., Reneman, L., 2015. Effects of long-term methylphenidate treatment in adolescent and adult rats on hippocampal shape, functional connectivity and adult neurogenesis. Neuroscience 309, 243–258.

Volkow, N.D., Fowler, J.S., Wang, G.J., Ding, Y.S., Gatley, S.J., 2002. Role of dopamine in the therapeutic and reinforcing effects of methylphenidate in humans: results from imaging studies. Eur. Neuropsychopharmacol. 12, 557–566.

Wu, H., Deng, R., Chen, X., Wong, W.C., Chen, H., Gao, L., Nie, Y., Wu, W., Shen, J., 2016. Caveolin-1 is critical for lymphocyte trafficking into central nervous system during experimental autoimmune encephalomyelitis. J. Neurosci. 36, 5193–5199.

Yun, H.S., Park, M.S., Ji, E.S., Kim, T.W., Ko, I.G., Kim, H.B., Kim, H., 2014. Treadmill exercise ameliorates symptoms of attention deficit/hyperactivity disorder through reducing Purkinje cell loss and astrocytic reaction in spontaneous hypertensive rats. J. Exerc. Rehabil. 10, 22–30.

Zhang, J., Wang, X., Vikash, V., Ye, Q., Wu, D., Liu, Y., Dong, W., 2016. ROS and ROS-mediated cellular signaling. Oxid. Med. Cell Longev. 2016, 4350965. doi:10.1155/2016/4350965.

Zhang, S., Kan, Q.C., Xu, Y., Zhang, G.X., Zhu, L., 2013. Inhibitory effect of matrine on blood-brain barrier disruption for the treatment of experimental autoimmune encephalomyelitis. Med. Inflamm. 2013, 736085. doi:10.1155/2013/736085.